Available online at www.sciencedirect.com
ScienceDirect
Journal of the European Ceramic Society 29 (2009) 1157–1163
www.elsevier.com/locate/jeurceramsoc

The effect of Nb doping on dielectric and ferroelectric properties of PZT thin films prepared by solution deposition

Volkan Kayasu, Macit Ozenbas *

Department of Metallurgical and Materials Engineering, Middle East Technical University, 06531 Ankara, Turkey

Received 26 January 2008; received in revised form 24 July 2008; accepted 30 July 2008
Available online 21 September 2008

Abstract

Niobium (Nb)-doped lead zirconate titanate thin films (PNZT) were produced by solution deposition with nominal compositions, $Pb_{(1-0.5x)}(Zr_{0.53}Ti_{0.47})_{1-x}Nb_xO_3$ where $x = 0.00–0.07$. The effects of sintering temperature, sintering time, variation of thickness in the films and change of niobium content were investigated with regard to phase development, microstructure, and ferroelectric and dielectric characteristics. The best results were obtained in double-layered films (390 nm) sintered at 600 °C for 1 h. Optimum doping level was found in 1% Nb-doped films. For 1% Nb-doped $[Pb_{0.995}(Zr_{0.53}Ti_{0.47})_{0.99}Nb_{0.01}O_3]$ films, remanent polarization (P_r) of 35.8 μC/cm^2 and coercive field (E_c) of 75.7 kV/cm have been obtained. The maximum dielectric constant was achieved in 1% Nb-doped films which was 689. Ferroelectric and dielectric properties decreased at higher Nb doping levels because of the changes in the grain size and perovskite lattice parameters.
© 2008 Elsevier Ltd. All rights reserved.

Keywords: Solution deposition; Ferroelectric properties; Dielectric properties; PNZT

1. Introduction

Lead zirconate titanate (PZT) thin films that have a composition $Pb(Zr_{0.53}Ti_{0.47})O_3$, near the morphotropic phase boundary, have been investigated extensively in the recent years.[1,2] They have been used in ferroelectric memory applications and micro-electro-mechanical systems (MEMS).[3–6] The most common applications of PZT- and niobium-doped PZT thin films are accelerometers, ferroelectric random access memories (FeRAM), amplifiers, thermal imaging and non-volatile memories.

Ferroelectric thin films have many advantages over their bulk counterparts. Lower operating voltage, greater design flexibility and the ability to fabricate nano-level composites are the main benefits of thin films compared to the bulk materials.[7,8]

PZT materials which have a perovskite structure possess a number of properties which make them suitable candidates for memory applications.[6] With some compositional modifications like adding dopants, modifiers or using other compositions, the properties can be improved for specific applications.[9]

In the perovskite structure, Nb^{5+} substitutes for Zr^{4+}/Ti^{4+} site. By the substitution of Nb^{5+} ion on perovskite lattice, additional positive charge is introduced and Pb^{2+} vacancies are created to maintain charge neutrality. For every two atoms of Nb^{5+} introduced into the lattice, one Pb^{2+} vacancy occurs. Such Nb-doped PZT materials have been reported to possess increased dielectric constants, lower coercive fields and square hysteresis loops.[6,10,11] Haccart et al. found that dielectric constant (ε_r) increases from 800 for the undoped PZT film to a maximum value of 1100 for a PNZT film containing 2% Nb. Maximum and remnant polarizations are also improved with 2% Nb introduction.[10] Souza et al. indicated that 1% Nb-doped PNZT thin films show higher remnant polarization ($P_r = 20$ μC/cm^2) compared to pure PZT thin films and the coercive field ($E_c = 60.0$ kV/cm) is lower than the pure PZT thin films ($E_c = 126.0$ kV/cm).[10] On the other hand, Shimizu et al. claimed that remnant polarization and coercive field values of the PNZT thin films decreased as the Nb contents increased from 2.8 to 4.2% and no optimum value was found.[12]

For the production of PNZT thin films, numerous deposition techniques are used such as chemical solution deposition, sputtering, pulsed laser deposition (PLD) and molecular beam epitaxy (MBE).[9] Chemical solution deposition processes for the production of ferroelectric thin films have many advantages over

* Corresponding author. Tel.: +90 312 210 2532; fax: +90 312 210 2518.
E-mail address: ozenbas@metu.edu.tr (M. Ozenbas).

0955-2219/$ – see front matter © 2008 Elsevier Ltd. All rights reserved.
doi:10.1016/j.jeurceramsoc.2008.07.062

other production methods and it was used in the entire study. Control of chemical composition and microstructure, low cost and high chemical homogeneity are some of the gains of using chemical solution deposition method.

There were many studies about Nb addition on PZT, but only few of them used solution deposition method. Also, in most of the studies, dielectric, ferroelectric properties and fatigue characteristics were handled separately. The reported results are generally scattered as indicated above. In this study, the results were discussed from all aspects and consistent explanations will be given by considering all of the parameters. Nb-doped PZT thin films were produced by preparing a homogeneous solution and then forming a crack-free and smooth film on (1 1 1)-Pt/Ti/SiO_2/Si-(1 0 0) substrates. The optimum sintering conditions and thicknesses of the films were determined using XRD, SEM and results of electrical measurements. The effect of Nb addition on ferroelectric and dielectric properties was investigated, together with leakage current analysis of PNZT thin films.

2. Experimental procedure

Solutions used to produce PNZT thin film were obtained with respect to the nominal compositions, $Pb_{(1-0.5x)}(Zr_{0.53}Ti_{0.47})_{1-x}Nb_xO_3$: $x = 0.00$–0.07. Compositions were chosen near the morphotropic phase boundary (MPB) [Zr/Ti: 53/47] to maximize the dielectric and ferroelectric properties of the films. To obtain the final form of the film, solution preparation, coating and heat treatment processes were carried out, respectively.

The starting materials used for preparing the precursors were lead acetate trihydrate $Pb(CH_3COO)_2{\cdot}3H_2O$ (Aldrich Co., purity 99+%), titanium(IV) isopropoxide $Ti[(CH_3)_2CHO]_4$ (Aldrich Co., purity 97%), zirconium(IV) propoxide $Zr(C_3H_7O)_4$ (Aldrich Co., 70 wt.% solution in 1-propanol), and niobium(V) ethoxide $Nb(OC_2H_5)_5$ (Aldrich Co., purity 99.95%). The solvent used during the study was 2-methoxyethanol $C_3H_8O_2$ (Aldrich Co., purity 99%). Deionized water was used as a diluting solvent.

To obtain a homogeneous solution with the desired composition, two different solutions were prepared in a method similar to that reported by Budd et al.[13] and then mixed with each other. The concentration and the volume of the solutions were set to 0.4 M and 40 ml. In the first solution, lead acetate trihydrate, niobium(V) ethoxide and 2-methoxyethanol were mixed and heated to 90 °C. Lead acetate trihydrate was taken 10% excess to compensate the losses during the sintering process. In the second solution, zirconium(IV) propoxide, titanium(IV) isopropoxide and 2-methoxyethanol were mixed at room temperature. Also, titanium(IV) isopropoxide was taken 10% excess due to its volatilization during the preparation of the precursor.

All of the PNZT and PZT films were coated on (1 1 1)-Pt/Ti/SiO_2/Si-(1 0 0) substrates. The similarities in thermal expansion coefficients and lattice parameter make Pt a good choice for the bottom electrode.[6] They were cut from the wafers with the dimensions of 1.5 cm to 1.5 cm and then rinsed in acetone for cleaning. Spinning rate of the spin coater was set to 1500 rpm for 30 s. To achieve the required thickness, multiple coating-pyrolysis cycles were employed and single and multilayered films up to four layers have been produced.

The films were heated to 150 °C for 15 min for the removal of water as the drying process. The next step was to heat the films to 450 °C and keep them for 15 min at that temperature for the removal of organics. After the drying and pyrolysis steps, sintering process was performed. This step is critical because of the crystallization of the amorphous phase and the formation of other phases. Sintering temperature and time were selected as two important parameters in this study. They affect the ferroelectric and dielectric properties of the films because of the changes occurring in the film during the sintering process. To understand the effects of sintering temperature and find the optimum temperature for the sintering process, three different temperatures were chosen as 600, 650 and 700 °C.[2,5,14–16] Also the sintering times for the films were taken as 1, 2 and 3 h. All of the possible combinations were applied to find the optimum conditions for sintering.

For the chemical and microstructural analysis of the films, JEOL JSM-6400 scanning electron microscope (SEM) was used. Thickness measurements were carried out using the cross-sectional SEM images of the films. X-ray diffraction analysis were performed using a Rigaku D/MAX 2200/PC diffractometer between angles 20° and 60° (2θ) with Cu(Kα) radiation. Surface characteristics of the films were measured by Nanosurf Easyscan 2 Atomic Force Microscopy (AFM). Thermal measurements were carried out by Setaram Labsys TGA/DTA unit to determine the critical temperatures and the weight losses occurred during the heating of the solution using powders prepared by keeping the PNZT solution at 100 °C for 5 h. These powders were then heated to 900 °C with a heating rate of 10 °C/min. Grain size of the films was found by using the SEM images obtained by FEI Quanta 400 FEG Field Emission Scanning Electron Microscope (FESEM). Viscosity of the solutions was found by using TA Instruments ARES Rheometer. Ferroelectric and dielectric properties were evaluated by using a Radiant Ferroelectric Tester Precision LC (Radiant Technologies, Inc.) and Impedance Analyzer (Agilent 4294A), respectively. Leakage current analysis was also carried out using Radiant Ferroelectric Tester.

3. Results and discussion

3.1. Characterization of PNZT solution

Fig. 1 shows the differential thermal analysis (DTA) and thermogravimetry (TG) curves for a PNZT gel precursor of composition $Pb_{0.985}(Zr_{0.53}Ti_{0.47})_{0.97}Nb_{0.03}O_3$. The exothermic peak at 318 °C can be explained by the decomposition of light organics and acetates that is supported by the second weight loss region in the TGA curve. The formation of the inorganic ceramic phase and the decomposition of organic compounds had occurred at ≤600 °C. Final TGA weight loss occurs at ∼580 °C which coincides with crystallization DTA peak at 580 °C. Further increase in the temperature only promotes the crystallization because there is no weight losses observed after 580 °C. The selection of pyrolysis temperature as 450 °C and the sintering temperature

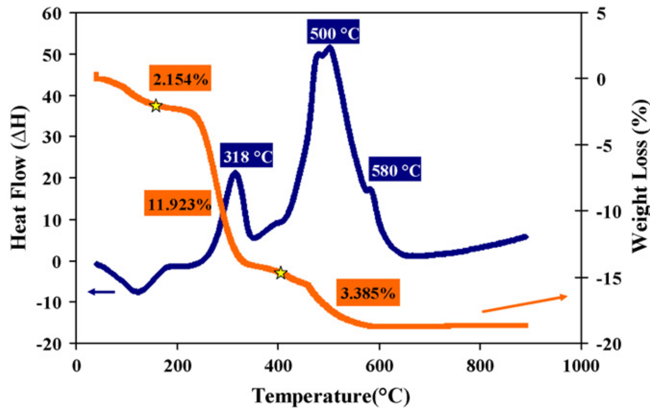

Fig. 1. Differential thermal analysis (DTA) and thermogravimetry (TG) curves of PNZT gel precursor of composition $Pb_{0.985}(Zr_{0.53}Ti_{0.47})_{0.97}Nb_{0.03}O_3$.

as 600 °C was a good choice for both the perovskite formation and to obtain crack-free and smooth films. It was found that, Nb doping level has no effect on the TGA plot. This result is also supported by the study of Kurchania et al.[1]

3.2. Characterization of PNZT thin films

Optimum sintering temperature and sintering duration were estimated by determining the phases present in the film and the changes in the peak intensities of these phases. XRD results for PNZT thin films having the composition $Pb_{0.985}(Zr_{0.53}Ti_{0.47})_{0.97}Nb_{0.03}O_3$ and thickness of 390 nm were used to estimate the optimum sintering parameters.

The final crystal structure of the PNZT thin films was highly sensitive to both the initial chemical stoichiometry and sintering temperature. The volume fraction of pyrochlore phase and the time required for its transformation to the perovskite phase strongly depend on temperature.[6] After sintering at 450 °C for 3 h, Pt(1 1 1) and PbO peaks were determined at $2\theta = 40.0°$ and $2\theta = 29.5°$, respectively. Kurchania et al.[1] found the same PbO peak with the PNZT films sintered at 500 °C. Fig. 2(a) shows that there was only perovskite phase in the films sintered at 600 °C and no impurity phase was determined. This result is consistent with the previous studies.[11,17] An additional faint peak was observed in XRD patterns of films sintered at temperatures higher than 600 °C (Fig. 2(a)). The origins of this peak are uncertain, but one possibility is that it is due to the interdiffusion of Ti adhesion layer at the higher process temperatures. This extra peak may tentatively be assigned to a Ti_2O_3 phase, for which the JCPDS file of 76-0145 indicates a diffraction angle of $2\theta = 33.1°$. These results, therefore, yielded the optimum sintering temperature as 600 °C. The optimum sintering time was determined as 1 h using the intensities of the perovskite peaks at 600 °C together with the results obtained from ferroelectric and dielectric measurements.

PNZT thin films with different compositions were produced upon the determination of optimum sintering parameters. Nb content was changed at constant sintering temperature, sintering time and film thickness in order to observe the effects of Nb^{5+} ion addition on PZT thin films. To make a comparison

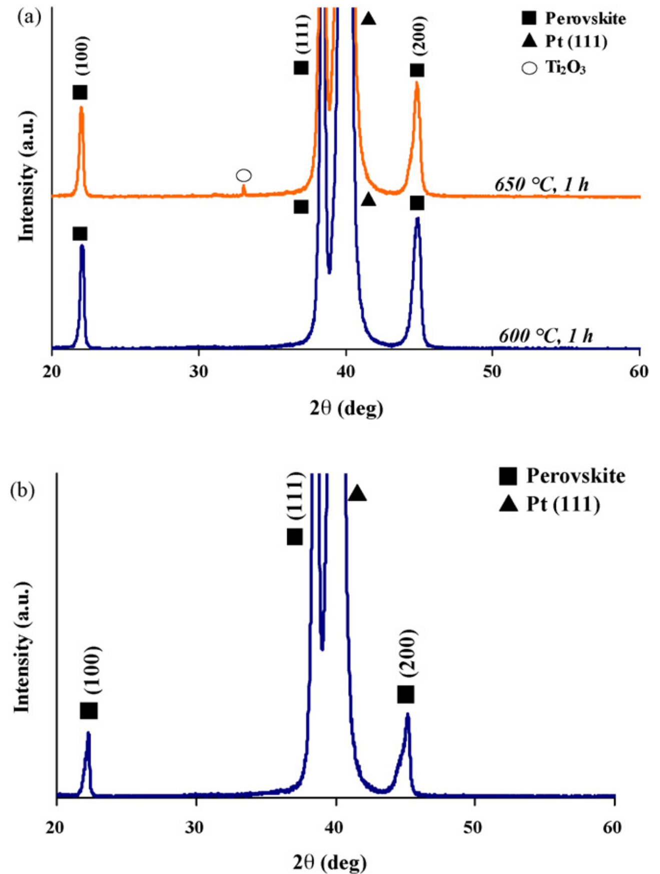

Fig. 2. X-ray spectra of PNZT thin films that are 390 nm with the composition: (a) $Pb_{0.985}(Zr_{0.53}Ti_{0.47})_{0.97}Nb_{0.03}O_3$ sintered at 600 and 650 °C for 1 h and (b) $Pb_{0.995}(Zr_{0.53}Ti_{0.47})_{0.99}Nb_{0.01}O_3$ and sintered at 600 °C for 1 h.

of PNZT thin films, undoped PZT films were also produced. Fig. 2(b) shows the X-ray spectra of a PNZT thin film with the composition $Pb_{0.995}(Zr_{0.53}Ti_{0.47})_{0.99}Nb_{0.01}O_3$ (1% Nb doping). The highest perovskite peak emerges at $2\theta = 38.0°$ (1 1 1) showing that the preferred orientation was on (1 1 1) crystallographic plane. Pt(1 1 1) peak was observed at $2\theta = 40.0°$. The intensities of the perovskite peaks (1 0 0), (1 1 1) and (2 0 0) were highest in the 1% Nb-doped films. Overall XRD data shows that as the Nb addition was increased, the intensities of the perovskite peaks were decreased due to the fact that the incorporation of Nb makes it more difficult to produce films that have single-phase perovskite XRD patterns. Other workers have also reported lower levels of perovskite intensities with increased Nb concentration in PNZT films.[1,2]

3.3. Morphology of PNZT thin films

To achieve an optimum thickness value, single and multilayered films up to four layers were produced. Optimum thickness achieved in double layered films, because single layered films break at voltages higher than 5 V and thicker films are not wanted in our study. Fig. 3 shows the thickness and the uniformity of a double-layered film. In this micrograph the PNZT thin film with a thickness of 390 nm is shown. The thickness was measured as 250 nm in single layered films. Three and four layered films

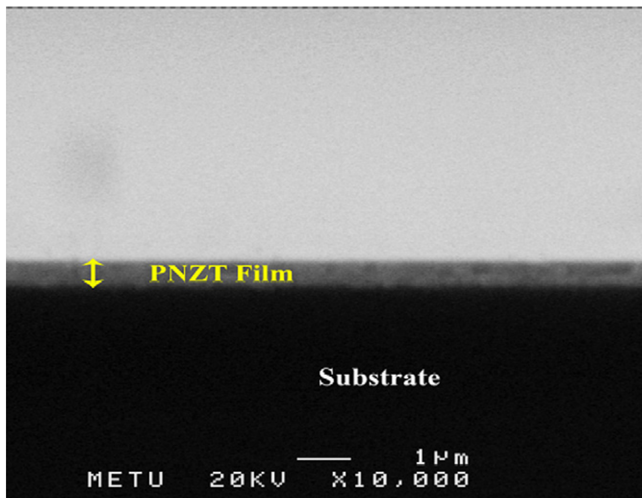

Fig. 3. SEM micrograph of PNZT thin film with the composition of $Pb_{0.985}(Zr_{0.53}Ti_{0.47})_{0.97}Nb_{0.03}O_3$ and sintered at 600 °C for 1 h.

had a thickness of 520 and 870 nm, respectively. Fig. 4(b) shows the FESEM image of 1% Nb-doped PNZT thin film that has a thickness of 390 nm and sintered at 600 °C for 1 h. The average grain size was determined as 113 ± 0.7 nm by quantitative metallographic methods.[18] It is found in the literature that, the grain size of PNZT films changes between 100 and 200 nm.[1,2,10] The use of Pt as a substrate allows for easy nucleation of the perovskite phase because of the approximate lattice parameters of $PbTiO_3$ and Pt.[2] Since Ti makes nucleation easier and Nb^{5+} substitutes for Zr^{4+} in some proportion, the surface number density of nuclei increases in PNZT thin films leading to a fine grained perovskite structure.[2,10,11] For the undoped PZT films, grain size of 85 ± 1.1 nm is achieved that is seen from Fig. 4(a). For 3 and 5% Nb doping, grain sizes of 104 ± 1.4 nm and 69 ± 1.2 nm, respectively, were obtained. Fig. 4(c) shows the grains of the PNZT thin film with 3% Nb. For 7% Nb-doped PNZT films, the grains could not be detected because of the defects and very fine pyrochlore phase at the film surface.[1] Grain size decreases with increasing Nb content starting from 1% Nb addition. This can be explained by the previous studies that, Nb is an effective grain growth inhibitor.[19,20]

3.4. Dielectric properties of PNZT thin films

Dielectric constant (ε_r) and loss tangent ($\tan\delta$) values of the PNZT thin films were measured in the frequency range 1–500 kHz with an oscillation voltage of 0.05 V in order to compare the dielectric properties.

Fig. 5 shows the change of dielectric constant values at 1 kHz with respect to Nb concentration. The double layered PNZT thin films (390 nm) were sintered at 600 °C for 1 h for all compositions. For the undoped films, a dielectric constant of 502 was obtained. For 1% Nb doping, the maximum dielectric constant value was reached as 689. For higher doping concentrations (>1%), dielectric constant decreases almost linearly. Other workers[1,2,11,17,21] also stated that for low Nb concentrations dielectric constant reaches a maximum point and for higher Nb doping levels ε_r decreases. A similar result was also found by Klissurska et al., in sol–gel-derived 300 nm thick PNZT films containing 1% Nb yielding the maximum dielectric constant value ~740 and their 600 °C sintered samples showed a strong decrease in dielectric constants with Nb doping.[2] The

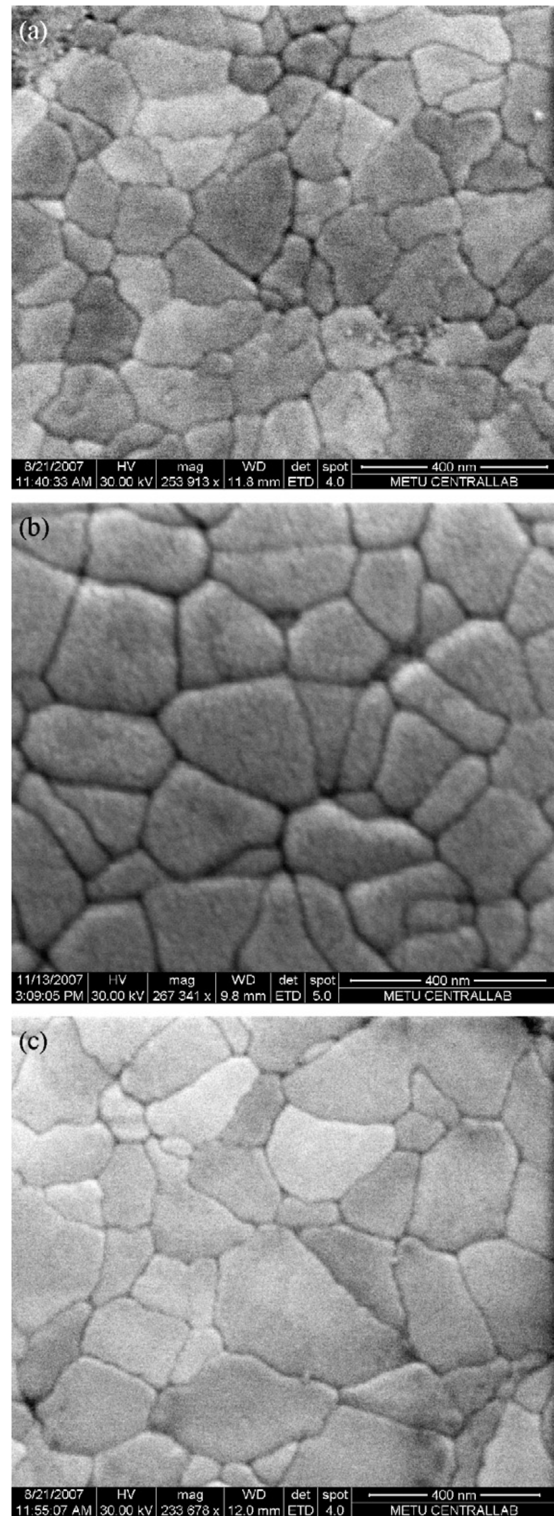

Fig. 4. FESEM images for PNZT thin films of composition: (a) $Pb(Zr_{0.53}Ti_{0.47})O_3$, (b) $Pb_{0.995}(Zr_{0.53}Ti_{0.47})_{0.99}Nb_{0.01}O_3$ and (c) $Pb_{0.985}(Zr_{0.53}Ti_{0.47})_{0.97}Nb_{0.03}O_3$ sintered at 600 °C for 1 h.

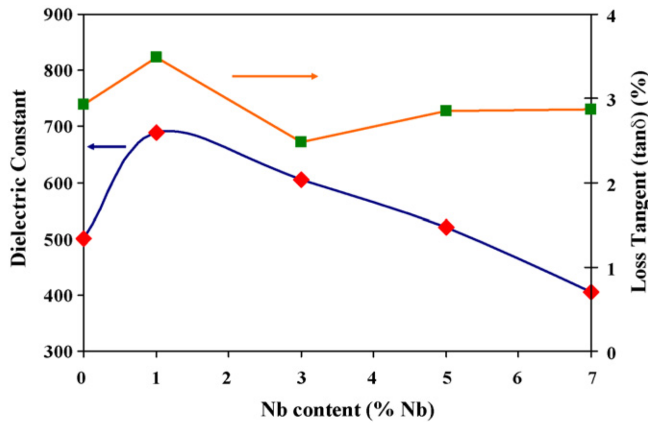

Fig. 5. Change of dielectric constant (ε_r) and loss tangent ($\tan\delta$) values of PNZT thin films at 1 kHz with varying Nb content while the sintering temperature, sintering time and thickness were held constant.

increase in ε_r in 1% Nb-doped PNZT films could be explained by the grain growth of the PNZT films with respect to undoped films. We observed an increase of grain size from 85 ± 1.1 nm in undoped film to 113 ± 0.7 nm in 1% Nb-doped film. The dielectric constant of Nb-doped PZT films is very sensitive to the grain size.[11] Particularly the domain wall mobility depends on the microstructure. When grain size starts to decrease as seen in our study above 1% Nb doping, the density of domains increases and so their mobility is reduced. A lattice distortion appears with the Nb addition in the perovskite lattice which significantly changes the lattice parameters.[20] These factors could be the cause of the decrease in dielectric constant values in our samples containing more than 1% Nb. Fig. 5 also shows the change of loss tangent with varying Nb content. It can be seen that the loss tangent values lie between 2 and 4% indicating that Nb doping has almost no effect on loss tangent values which is also given by Haccart et al.[11] The maximum loss tangent values in our study were reached for 1% Nb doping as 3.5%.

Fig. 6(a) shows the effect of thickness on dielectric constant. Dielectric constant increases with increasing thickness except for 3-layered (520 nm) PNZT thin film. The maximum value was achieved for 4-layered films (870 nm) as 1275. This increase is consistent with the previous studies.[6,21,22] The increase in dielectric constant can be explained by formation of denser films (Fig. 6(b)) because, number of layers and pyrolysis cycles increases as the thickness increases. Increased number of layers leads to a decrease in film porosity in solution deposition technique since subsequent layers coated on the former pyrolysed layer covers up the pores and bulk defects left behind by the organic burn-off.[22]

3.5. Ferroelectric properties of PNZT thin films

Ferroelectric properties of PNZT thin films were measured by comparing the hysteresis parameters like remnant polarization (P_r) and coercive field (E_c). Table 1 shows the P_r and E_c values of the PNZT thin films having a composition of $Pb_{0.985}(Zr_{0.53}Ti_{0.47})_{0.97}Nb_{0.03}O_3$. All of the films were 390 nm in thickness and voltage applied to the films was ranging from

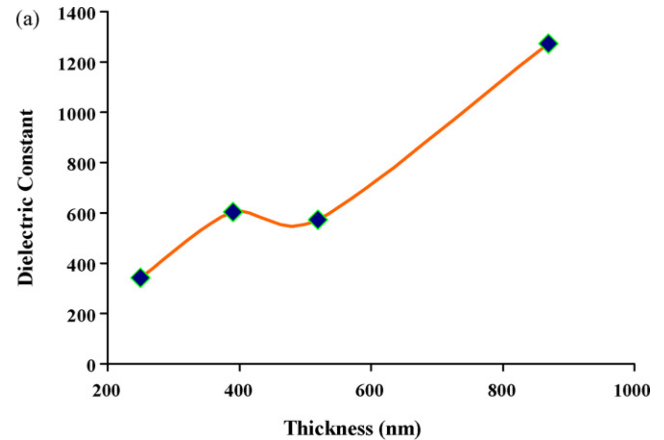

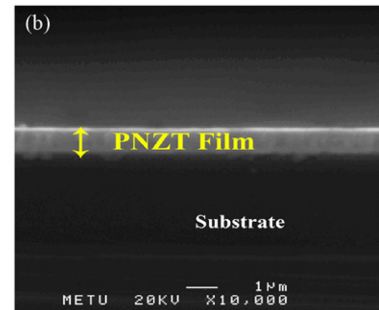

Fig. 6. (a) Change of dielectric constant with changing thickness graph. The composition of the PNZT film is $Pb_{0.985}(Zr_{0.53}Ti_{0.47})_{0.97}Nb_{0.03}O_3$ and it was sintered at 600 °C for 1 h. (b) SEM micrograph of PNZT thin film with composition of $Pb_{0.985}(Zr_{0.53}Ti_{0.47})_{0.97}Nb_{0.03}O_3$ and sintered at 600 °C for 1 h that has a thickness of 870 nm.

−5 to +5 V. For PNZT thin films, saturation of the hysteresis loops could not be achieved with the maximum applied field of 382 kV/cm (15 V). The highest P_r value was found as 13.7 μC/cm^2 for the films sintered at 600 °C for 1 h as supported by XRD studies which yield pure perovskite phase for films sintered at the same conditions. Measured P_r and E_c values were varying for different sintering conditions. E_c of 42.2 kV/cm was obtained for the films sintered at 600 °C for 1 h. Ferroelectric properties of the films with different compositions were measured at 5 V after the determination of optimum sintering parameters for PNZT films as 600 °C and 1 h. Fig. 7 shows the hysteresis curves for PNZT thin films sintered at 600 °C for 1 h and had a thickness of 390 nm. All of the parameters except Nb content were kept constant in order to analyze the effect of Nb addition on PZT films. It was observed, in all of the films, that there is an asymmetry of the hysteresis loop on

Table 1
Remnant polarization (P_r) and coercive field (E_c) values of PNZT thin films (390 nm) having a composition of $Pb_{0.985}(Zr_{0.53}Ti_{0.47})_{0.97}Nb_{0.03}O_3$ taken at an applied voltage of 5 V

Temperature (°C)	Time (h)	P_r (remnant polarization) (μC/cm^2)	E_c (coercive field) (kV/cm)
600	1	13.7	42.2
	2	3.9	12.1
	3	7.4	20.4

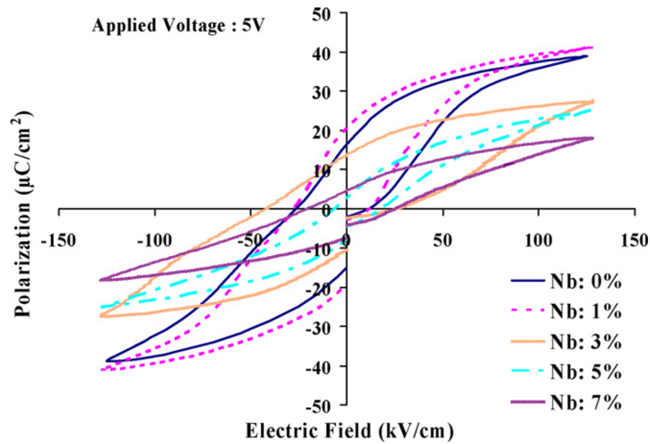

Fig. 7. Change of hysteresis behavior with varying Nb content for PNZT thin films sintered at 600 °C for 1 h with a thickness of 390 nm.

the electric field axis. The same behavior is also observed by other workers.[10,11,14] This shift can be named as internal electric field (E_{int}) or internal bias field. It is stated that the reason of the asymmetric behavior in PZT and PNZT films is due to the space charges.[10,11] Fig. 8 shows the change of remnant polarization and coercive field values with respect to Nb content. For the undoped PZT thin films, P_r and E_c values were found as 16.3 μC/cm^2 and 26.2 kV/cm, respectively. P_r increased to 20.6 μC/cm^2 for 1% Nb-doped PNZT films. Higher doping levels of more than 1% Nb decreases ferroelectric properties. It is observed that after 3% doping, the remnant polarization values are far below the undoped PZT thin films. Coercive field values are very close for the undoped and 1%-doped PNZT thin films. E_c value is increasing between 1 and 3% Nb-doped film. Kurchania et al.[1] observed that as the Nb content increased the coercive field had also increased, but the increase was small as compared to our results. Most of the studies found that Nb doping decreases coercive field.[6,10,11] Some of them stated that there is no effect of Nb doping on the coercive field.[12,14] These contradictory results show that, influence of Nb addition on coercive field is not well understood yet. After 3% Nb doping, coercive field decreased to 6.4 kV/cm and it increases back to 20.4 kV/cm for 7% Nb-doped films. The optimum Nb doping level was determined as

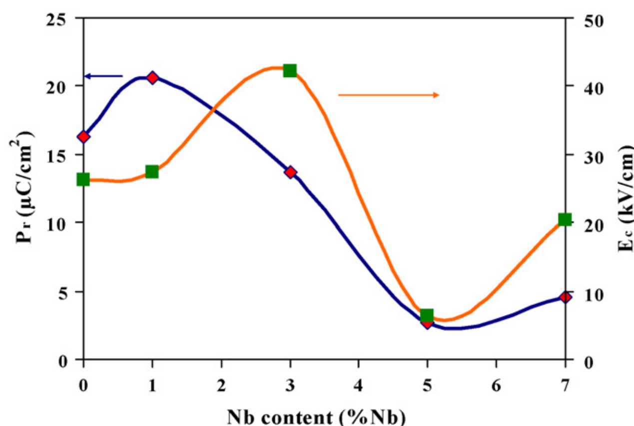

Fig. 8. Change of remnant polarization (P_r) and coercive field (E_c) with respect to Nb content.

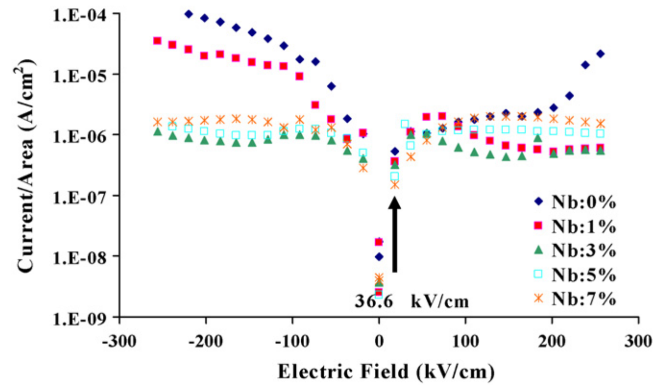

Fig. 9. Leakage current analysis (*J*–*E*) for PNZT thin films with varying Nb content while other parameters were held constant.

1% and the same results were also achieved by Klissurska et al.[14]

3.6. Leakage current analysis of PNZT thin films

Fig. 9 shows the influence of Nb doping on the current density. The leakage current densities of the PNZT thin films were compared at 36.6 kV/cm. For the undoped PZT film, it is 1.1×10^{-6} A/cm^2. As the Nb content increases, current density decreases and reaches to 4.4×10^{-7} A/cm^2 for the 7% Nb-doped film. Similar results were obtained by other studies.[1,10,23] This decrease can be explained by the addition of a higher valence Nb^{5+} cation to the perovskite matrix. By this way, excess oxygen vacancies are created and compensated by combining free electrons. The increase of barrier height to thermonic emissions of electrons from the Pt electrode makes it difficult for electrons to transfer from Pt electrode into PNZT film because of the decreased electron concentration.[24]

4. Conclusions

The effect of Nb doping on PZT [Zr/Ti: 53/47] thin films were studied through the preparation of PZT and PNZT thin films by sol–gel method and coating of them on (1 1 1)-Pt/Ti/SiO_2/Si-(1 0 0) substrates. Different parameters like sintering temperature, sintering time, Nb content and film thickness were selected to find the optimum properties of the films. Comparison of the PNZT thin films were carried out by investigating the structural and electrical properties of the films.

PNZT thin films that are smooth and crack-free were grown on platinised silicon substrates by a spin coating process and optimum film thickness was achieved as 390 nm (double layered films). The optimum Nb doping was achieved for the films that have 1% Nb and has a composition of $Pb_{0.995}(Zr_{0.53}Ti_{0.47})_{0.99}Nb_{0.01}O_3$. The optimum sintering conditions were determined as 600 °C and 1 h. Grain size decreases with increasing Nb content except for 1% Nb-doped films which have a grain size of 113 ± 0.7 nm. Dielectric measurements showed that, maximum dielectric constant was achieved for 1% Nb-doped films as 689. This value decreased as the Nb content was further increased. Loss tangent values were found between

2 and 4% and independent of Nb concentrations. Ferroelectric measurements also supported dielectric measurements. Maximum remnant polarization was found as 35.8 $\mu C/cm^2$ for 1% Nb-doped films using 15 V (382 kV/cm) applied voltage.

Acknowledgements

This work was supported by Scientific and Technological Research Council of Turkey (TUBITAK) through the project 106M060. TG/DTA, viscosity, dielectric and FESEM measurements were conducted at the Central Laboratory of Middle East Technical University.

References

1. Kurchania, R. and Milne, S. J., Effect of niobium modifications to PZT (53/47) thin films made by a sol–gel route. *J. Sol–Gel Sci. Technol.*, 2003, **28**, 143–150.
2. Klissurska, R. D., Brooks, K. G., Reaney, I. M., Pawlaczyk, C., Kosec, M. and Setter, N., Effect of Nb doping on the microstructure of sol–gel-derived PZT thin films. *J. Am. Ceram. Soc.*, 1995, **78**(6), 1513–1520.
3. Nistorica, C., Zhang, J., Padmini, P., Kotru, S. and Pandey, R. K., Integrated PNZT structures for MEMS gyroscope. *Integr. Ferroelectr.*, 2004, **63**, 49–54.
4. Kwok, K. W., Kwok, K. P., Tsang, R. C. W., Chan, H. L. W. and Choy, C. L., Preparation and piezoelectric properties of sol–gel-derived Nb-doped PZT films for MEMS applications. *Integr. Ferroelectr.*, 2006, **80**, 155–162.
5. Kim, W. S., Ha, S. M., Park, H. H. and Kim, C. E., The effects of cation-substitution on the ferroelectric properties of sol–gel derived PZT thin film for FRAM application. *Thin Solid Films*, 1999, **355–356**, 531–535.
6. Ryder Jr., D. F. and Raman, N. K., Sol–gel processing of Nb-doped $Pb(Zr,Ti)O_3$ thin films for ferroelectric memory applications. *J. Electron. Mater.*, 1992, **21**(10), 971–975.
7. Larsen, P. K., Cuppens, R. and Spierings, G. A. C. M., Ferroelectric memories. *Ferroelectrics*, 1992, **128**, 265–292.
8. Uhlmann, D. R., Dawley, J. T., Poisl, W. H., Zelinski, B. J. J. and Teowee, G., Ferroelectric films. *J. Sol–Gel Sci. Technol.*, 2000, **19**, 53–64.
9. Buchanan, R. C., *Ceramic Materials for Electronics*. Marcel Dekker, New York, 1991, pp. 150–152.
10. Souza, E. C. F., Simoes, A. Z., Cilense, M., Longo, E. and Varela, J. A., The effect of Nb doping on ferroelectric properties of PZT thin films prepared from polymeric precursors. *Mater. Chem. Phys.*, 2004, **88**, 155–159.
11. Haccart, T., Remiens, D. and Cattan, E., Substitution of Nb doping on the structural, microstructural and electrical properties in PZT films. *Thin Solid Films*, 2003, **423**, 235–242.
12. Shimizu, M., Fujisawa, H. and Shiosaki, T., Effects of La and Nb modification on the electrical properties of $Pb(Zr,Ti)O_3$ thin films by MOCVD. *Integr. Ferroelectr.*, 1997, **14**, 69–75.
13. Budd, K. D., Dey, S. K. and Payne, D. A., Sol–gel processing of $PbTiO_3$, $PbZrO_3$, PZT and PLZT thin films. *Br. Ceram. Soc. Proc.*, 1985, **36**, 107–121.
14. Klissurska, R. D., Tagantsev, A. K., Brooks, K. G. and Setter, N., Use of ferroelectric hysteresis parameters for evaluation of niobium effects in lead zirconate titanate thin films. *J. Am. Ceram. Soc.*, 1997, **80**(2), 336–342.
15. Tohge, N., Takahashi, S. and Minami, T., Preparation of $PbZrO_3$–$PbTiO_3$ ferroelectric thin films by the sol–gel process. *J. Am. Ceram. Soc.*, 1991, **74**(1), 67–71.
16. Tuttle, B. A., Doughty, D. H. and Martinez, S. L., Microstructure of solution-processed lead zirconate titanate (PZT) thin films. *J. Am. Ceram. Soc.*, 1991, **74**(6), 1455–1458.
17. Haccart, T., Cattan, E., Remiens, D., Hiboux, S. and Muralt, P., Evaluation of niobium effects on the longitudinal piezoelectric coefficients of $Pb(Zr,Ti)O_3$ thin films. *Appl. Phys. Lett.*, 2000, **76**(22), 3292–3294.
18. Vander Voort, G. F., *Metallography, Principles and Practice*. McGraw-Hill, New York, 2004, p. 436.
19. M'peko, J. C., Peixoto, A. G., Jimenez, E. and Gaggero-Sager, L. M., Electrical properties of Nb-doped PZT 65/35 ceramics: influence of Nb and excess PbO. *J. Electroceram.*, 2005, **15**, 167–176.
20. Pereira, M., Peixoto, A. G. and Gomes, M. J. M., Effect of Nb doping on the microstructural and electrical properties of the PZT ceramics. *J. Eur. Ceram. Soc.*, 2001, **21**, 1353–1356.
21. Remiens, D., Cattan, E., Soyer, C. and Haccart, T., Piezoelectric properties of sputtered PZT films: Influence of structure, microstructure, film thickness (Zr,Ti) ratio and Nb substitution. *Mater. Sci. Semicond. Proc.*, 2003, **5**, 123–127.
22. Nayak, M., Lee, S. Y. and Tseng, T., Electrical and dielectric properties of $(Ba_{0.5}Sr_{0.5})$ TiO_3 thin films prepared by a hydroxide–alkoxide precursor-based sol–gel method. *Mater. Chem. Phys.*, 2003, **77**, 34–42.
23. Dimos, D., Schwartz, R. W. and Lockwood, S. J., Control of leakage resistance in $Pb(Zr,Ti)O_3$ thin films by donor doping. *J. Am. Ceram. Soc.*, 1994, **77**(11), 3000–3005.
24. Wang, S. Y., Cheng, B. L., Wang, C., Redfern, S. A. T., Dai, S. Y., Jin, K. J., Lu, H. B., Zhou, Y. L., Chen, Z. H. and Yang, G. Z., Influence of Ce doping on leakage current in $Ba_{0.5}Sr_{0.5}TiO_3$ films. *J. Phys. D. Appl. Phys.*, 2005, **38**, 2253–2257.